


Acupuncture Relieves Cervical Spondylosis Radiculopathy by Regulating Spinal Microglia Activation Through MAPK Signaling Pathway in Rats

Tianyu Shi ^{*}, Yitian Liu^{*}, Bo Ji, Jiajia Wang, Yunpeng Ge, Yang Fang, Yana Xie, Hongli Xiao, Le Wu, Yifei Wang

School of Acupuncture-Moxibustion and Tuina, Beijing University of Chinese Medicine, Beijing, People's Republic of China

^{*}These authors contributed equally to this work

Correspondence: Bo Ji, School of Acupuncture-Moxibustion and Tuina, Beijing University of Chinese Medicine, No. 11 North Third Ring East Road, Chaoyang District, Beijing, 100029, People's Republic of China, Tel +86 139 1180 6678, Email jibo678@163.com

Purpose: Local acupuncture has been found to have a good analgesic effect in rats with cervical spondylosis radiculopathy (CSR), but it lacks a regulatory effect on traditional Chinese medicine syndrome types of CSR. We proposed “Invigorating Qi and activating Blood” (IQAB) acupuncture, compared with Fenbid, and local electroacupuncture (LEA), to observe whether it has advantages in the protection of the CSR rat model and to elucidate its mechanism through the MAPK (mitogen-activated protein kinase) signaling pathway.

Materials and Methods: Male Sprague-Dawley rats were randomly divided into six groups: control, sham, model, Fenbid, LEA, and IQAB. The CSR model was induced by inserting nylon sutures to compress the C₄-T₁ nerve root. The Fenbid group was treated with ibuprofen sustained-release capsules (15 mg/kg·d, *ig*). The LEA group received electroacupuncture at both C₅ and C₇ EX-B2 once a day. The IQAB group received acupuncture at both ST36 and BL17 based on the LEA group's intervention. Mechanical allodynia and gait, morphological changes in the spinal cord, IL-6 and TNF- α levels, MAPKs phosphorylation ratio, monocyte chemoattractant protein-1 (MCP-1) levels in the spinal cord, and the expression of p-p38 in the spinal cord and its colocalization with neurons and glial cell activation markers were detected.

Results: Mechanical allodynia, gait disorder, edema, reduced Nissl-positive cell numbers, and increased IL-6 and TNF- α levels in the spinal cord were observed in CSR rats. IQAB significantly alleviated these changes, and the effects were generally comparable to those of Fenbid. Meanwhile, the phosphorylation ratios of p38 and extracellular regulated protein kinase (ERK), co-expression of p-p38 with neuron/microglia, and MCP-1 levels in the spinal cord were markedly down-regulated by IQAB compared with those in CSR model rats.

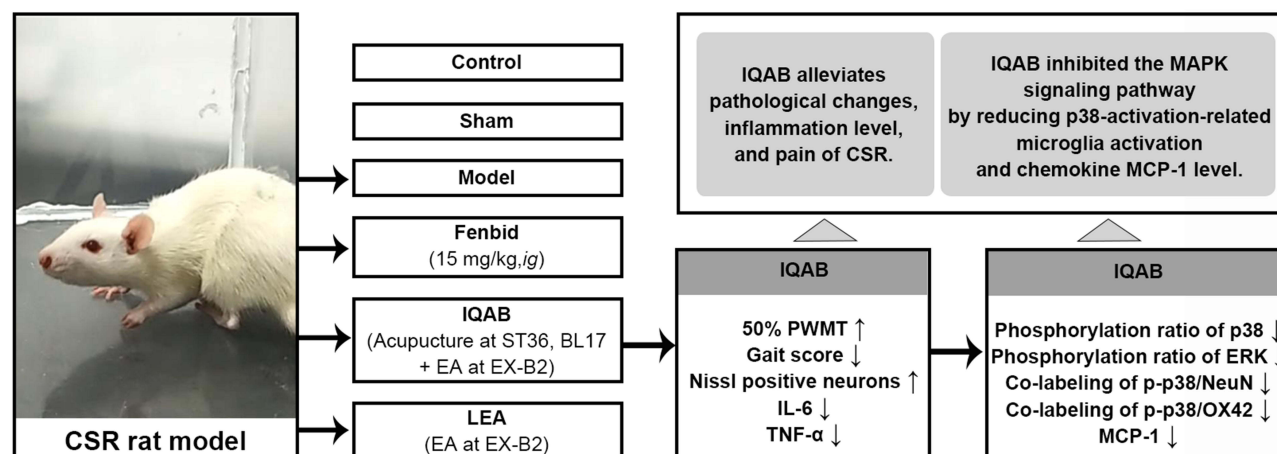
Conclusion: IQAB reduced p38-activation-related microglia activation and MCP-1 levels, thus alleviating pathological changes, inflammation levels in the local spinal cord, and pain behavior of CSR.

Keywords: analgesia, mitogen activated protein kinases, inflammatory cytokine, chemokine, MCP-1

Introduction

Among diseases affecting healthy life expectancy, neck and low back pain has soared from the 12th in 1990, to the 4th in 2015.¹ Incidences of cervical spondylosis radiculopathy (CSR) appear to be of increasing year by year, affecting younger age groups and occupational activities. Its prevalence in some areas is up to 10.6%.² CSR not only presents as radicular pain with sensory and motor changes but also causes sleep and emotional disorders, even requiring surgery in severe cases, wreaking people's quality of life.^{3,4}

Graphical Abstract



Medicines like NSAIDs, opiate, and relaxants could alleviate CSR symptoms and restore neurological function, but being limited by adverse reactions or addiction.⁵ Manipulation, instrument fixation, exercise, physiotherapy, and blocking are also used, but constrained by the ineffectiveness in long-term follow-up or serious complications.^{6–8} Acupuncture shows rapid relief of pain and numbness, whole body regulation, and minor adverse reactions, generally using local acupoints as the main points, and distant acupoints as adjunct points.^{9,10} Analgesic and neuroprotective mechanisms with local acupoints like “Cervical Jiaji” (EX-B2) have been reported in CSR models.^{11–13} However, according to TCM syndrome differentiation, disorders of the *Qi* and Blood form the main TCM syndrome type of CSR, accounting for 31.6%.¹⁴ A combination of local and dialectical acupoints is needed but has not received adequate attention. By reviewing the acupuncture RCTs, we also found that the most frequently selected adjunct points were BL17 and ST36, which regulate *Qi* and *Blood* balance, respectively. Thus, we formed the “Invigorating Qi and activating Blood” (IQAB) acupuncture method, compared with Fenbid and local electroacupuncture, to observe whether it has advantages in ameliorating pain and the inflammation level in the spinal cord, and explore its mechanism.

Under mechanical compression and chemical irritation to the nerve root, the inflammatory cascade in the spinal cord promotes the sensitization and maintenance of pain.¹⁵ Proinflammatory cytokines like TNF-α and IL-6 are important roles in this cascade.^{16,17} Mitogen-activated protein kinases (MAPKs), consisting of multiple parallel signal transduction pathways p38, c-Jun N-terminal kinase (JNK), and extracellular regulated protein kinase (ERK), can regulate allodynia development after nerve injury by regulating neural plasticity and inflammatory response.¹⁸ For example, p-p38 directly increases mediators like inflammation and cytokines,¹⁹ BDNF,²⁰ COX-2/PGE₂,²¹ and iNOS,²² reducing pain. P-JNK promotes the induction of chemokine monocyte chemoattractant protein-1 (MCP-1) in astrocytes to contribute to the central sensitization of neuropathic pain (NP).²³ P-ERK promotes the occurrence and maintenance of NP by activating ion channel proteins and transcription factors.¹⁸ Acupuncture can relieve radicular pain by decreasing IL-1β, IL-6, and TNF-α levels,^{13,24,25} and inhibiting ERK-related neuronal autophagy and apoptosis in the spinal cord.¹² However, the specific regulatory mechanisms remain unclear. Studies have shown that acupuncture can alleviate NP by regulating microglia/astrocyte activation regulated by MAPK and decreasing cytokines and chemokines produced by glial activation.^{26,27} However, it is unknown how acupuncture regulates glial cell activation through MAPK signaling pathways in the treatment of CSR. To clarify this, we tested the ratio of phosphorylated MAPKs, co-expression of phosphorylated MAPKs with different cellular markers, and level of MCP-1 in the spinal cord.

Materials and Methods

Animals

Forty-six male specific-pathogen-free (SPF) Sprague-Dawley (SD) rats (200 ± 10 g) were purchased from the Beijing Vital River Laboratory Animal Technology Co., Ltd. (certificate no. SCXK (Beijing) 2016-0006). The rats were housed at room temperature ($23 \pm 1^\circ\text{C}$) and relative humidity ($55 \pm 5\%$) with a light:dark cycle of 12:12 hours. Rats were maintained with free access to water and food. All animal experimental procedures complied with the National Institutes of Health's *Guide for the Care and Use of Laboratory Animals*. This study was approved by the Medicine and Animal Ethics Committee of Beijing University of Chinese Medicine (approval No. BUCM-4-2020090902-3039) on September 21, 2019.

Antibodies

For immunofluorescence, the primary antibodies were Phospho-p38 MAPK (Thr180/Tyr182) (D3F9) XP[®] rabbit mAb (4511S, 1:100, CST, MA, USA); Anti-CD11b + CD11c antibody [OX42] (ab1211, 1:100, Abcam, Cambridge, UK), anti-GFAP antibody [2A5] (ab4648, 1:50, Abcam), and NeuN (E4M5P) mouse mAb (94403S, 1:50, CST). The secondary antibodies used were Goat Anti-Rabbit IgG H&L (Alexa Fluor[®] 594) (ab150080, 1:400) and Goat Anti-Mouse IgG H&L (Alexa Fluor[®] 488) (ab150113, 1:400, Abcam).

The following primary antibodies were used for Western blotting: Rabbit Anti-p38 (phospho T180 + Y182) antibody (ab4822, 1:1000, Abcam), rabbit p38 MAPK Polyclonal antibody (14064-1-AP, 1:1000, Proteintech, IL, USA), Rabbit Phospho-ERK1/2 (Thr202/Tyr204) polyclonal antibody (28733-1-AP, 1:1000, Proteintech), Rabbit ERK1/2 Polyclonal antibody (16443-1-AP, 1:1000, Proteintech), phospho-SAPK/JNK (Thr183/Tyr185) (81E11) rabbit mAb (#4668, 1:500, CST), Rabbit SAPK/JNK Antibody (#9252, 1:1000, CST), and GAPDH Mouse Monoclonal antibody (600041-1-Ig, 1:25000, Proteintech). The secondary antibodies used were goat anti-mouse IgG HRP-linked antibody (ZB-2305, 1:10000, ZSXB Bio, Beijing, China) and goat anti-rabbit IgG HRP-linked antibody (ZB-2301, 1:10000, ZSXB Bio).

CSR Model and Grouping

After acclimatization for a week, we randomly selected six rats to form the control group; eight rats underwent the sham operation, and the remaining 32 rats underwent the modeling operation. The modeling surgery was performed as previously described.²⁸ Nylon sutures (0.5 mm diameter, 8 mm length) were prepared 1 day before modeling by soaking in 75% ethanol for 4 h and then immersing in 0.1% polylysine solution for 8 h. The rats were anesthetized with an intraperitoneal injection of 3% pentobarbital sodium solution (30 mg/kg body weight; Sigma-Aldrich) and fixed in the prone position. The hair on the back of the neck was shaved to create a 3 cm longitudinal incision from the T₂ spinous process upward. Careful blunt separation of the subcutaneous tissue and posterior cervical muscles was performed to minimize damage. The left C₆–C₇ vertebral arches were completely exposed and the muscles and ligaments on the bone surface were scraped. The ligamentum flavum and connective tissues in the intervertebral spaces were resected gently. The left C₆ and C₇ vertebral arches were then removed to expose the spinal cord. Two nylon sutures were implanted under the left nerve roots (from C₆ to T₁ and from C₇ to C₄) along the longitudinal axis of the spinal cord. Tissue closure was then performed layer by layer (Figure 1). For the sham group, the procedure was the same as described above, except that nylon sutures were not implanted. After surgery, the rats were intramuscularly injected with 50,000 units of penicillin sodium. On the 3rd day after the operation, 24 rats were successfully modeled, and 6 rats in the sham group were selected randomly according to the following criteria: 1) Before surgery, the rats had normal limb function without visible claudication, curling of the toes and claws, or joint stiffness. 2) After surgery, the scores of gait evaluation (by Kawakami's method) of the sham group were 1–2 and those of the model group were 2–3. 3) There were no symptoms of spinal cord compression. Then we randomly divided the 24 rats that met the model criteria into Model, Fenbid, Simple Local Electroacupuncture ("LEA") and IQAB groups, with six rats in each group (Figure 2A).

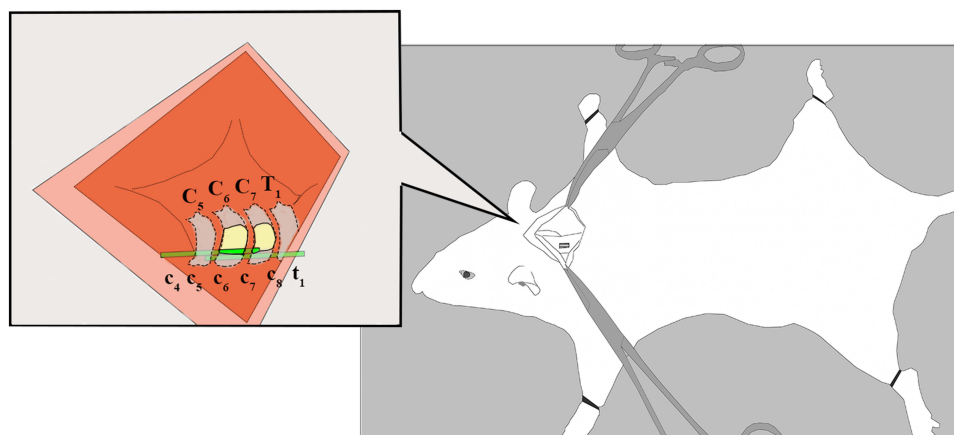


Figure 1 A diagram of CSR model surgery.

Notes: Two nylon sutures were individually implanted under the left nerve roots from C₆ to T₁ and from C₇ to C₄. The sutures were overlapped at the C₆ and C₇ nerve roots.

Abbreviations: C₅₋₇; T₁, spinal segment, c₄₋₈; t₁, nerve root segment.

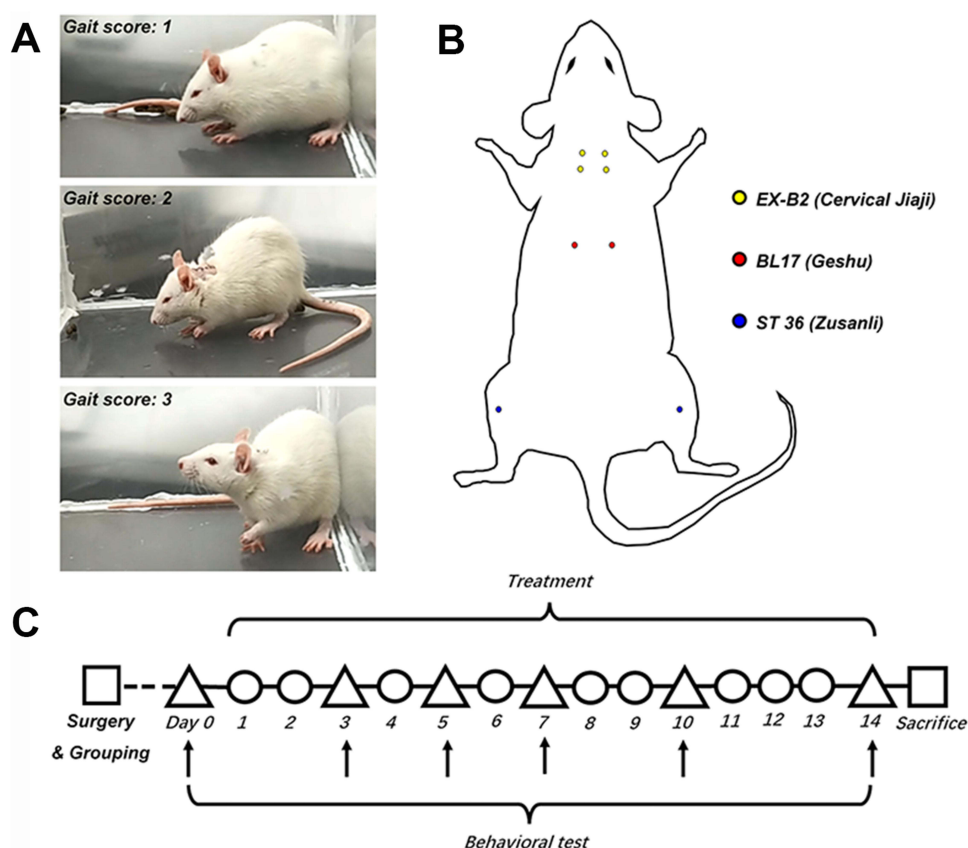


Figure 2 Gait evaluation, acupoints, and experimental procedure.

Notes: (A) Gait evaluation using Kawakami's method was used as both a grouping criterion and a behavioral test to evaluate intervention efficacy. (B) Bilateral acupoints C₅ and C₇ EX-B2 (Cervical Jiaji), BL17 (Geshu), and ST36 (Zusanli). In the LEA group, the rats were electroacupunctured at EX-B2, with two sets of electrodes connected at two ipsilateral points. In the IQAB group, the rats were acupunctured in the bilateral BL17 and ST36, combined using the same method as in the LEA group. (C) Brief flowchart of the experiment.

Drug Administration and Acupuncture

Interventions started on the 4th day after surgery. The Fenbid group was gavaged with Fenbid (GSK, Tianjin, China) dissolved in a saline solution with intake dose equivalent to ibuprofen 15 mg/kg·d. The other five groups were

administered saline solutions of the same volume by gavage. All groups were bound in a homemade restraint bag in a prone position, with the neck and limbs exposed at the same time every day. The LEA group was acupunctured in bilateral EX-B2 (3 mm lateral to the depression below the spinous process of the C₅ and C₇ vertebrae) at a depth of 8 mm using aseptic acupuncture needles (Hanyi, Beijing Hanyi Medical Instruments Co., Ltd., China). The needles at the ipsilateral C₅ and C₇ EX-B2 were connected to the same group of electrodes of the acupoint stimulation equipment (HANS-200A, Nanjing Jisheng Medical Technology Co., Ltd., China) with a 2/50 Hz sparse-dense wave, at 1.5 mA intensity, 30 min, once a day. In addition to undergoing the same acupuncture procedure as the LEA group, the IQAB group was acupunctured in bilateral BL17 (3 mm lateral to the depression below the spinous process of the T₇ vertebra) at a depth of 6 mm and bilateral ST36 (posterolateral to the knee joint, 5 mm below the fibula capitulum) at a depth of 7 mm (Figure 2B).

Behavioral Tests

The rats underwent neurobehavioral tests the day before and on the 3rd, 5th, 7th, 10th, and 14th day of the intervention (day 0, 3, 5, 7, 10, and 14). Mechanical allodynia was assessed using the 50% paw withdrawal mechanical threshold (PWMT) with eight von Frey filaments (Aesthesio, Danmic Global, USA). Rats were placed in a plexiglass cage with a steel wire mesh at the bottom. After acclimation to the test environment for 30 min, the rats were stimulated by filaments applied perpendicular to the surface of the front paws between the 3rd and 4th metacarpus. If the paw was withdrawn within 8 s or immediately after filament removal, it was considered positive. The interval between the two stimuli was longer than 10s. A sequence was recorded via the up-and-down method to calculate the 50% PWMT.²⁹ The rats were placed in a 30 × 30 × 25 cm plexiglass observation box to record their activities by video and analyze their gait according to the Kawakami method: 1) (normal gait with no forepaw deformities); 2) (normal gait with a marked forepaw deformity, such as flexed and/or inverted paws, or slight gait disturbance with a drop in the left forepaw), and 3) (severe gait disturbance with motor paresis of the ipsilateral left forepaw) (Figure 2A and C).³⁰

Histopathology

On the 15th day after the intervention began, the rats were euthanized after being anesthetized with an intraperitoneal injection of 3% pentobarbital sodium solution (60 mg/kg body weight; Sigma-Aldrich), and the C₄-T₁ spinal cord and the nerve roots connected to it were immediately removed and divided into two parts. One part was stored at -80°C for the following analysis. Another part was immersed in 4% paraformaldehyde dissolved in 0.1M PBS for 48 h, rinsed with tap water for 24 h, immersed in ascending gradient ethanol, xylene, and 65°C paraffin, then embedded in paraffin, making 4 μm serial sections. For Hematoxylin and Eosin (HE) staining, sections were deparaffinized in xylene and rehydrated in a descending gradient of ethanol, stained with hematoxylin for 10 min, washed three times with double-distilled water, 70% and 80% ethanol, eosin for 2.5 min, 95% and 100% ethanol, cleared with xylene, and mounted with neutral resins. For Nissl staining, after deparaffinization and rehydration, sections were stained with 56°C 1% Toluidine Blue for 40 min, washed three times with double distilled water, followed by ascending gradient ethanol and xylene, and mounted with neutral resins. All images were acquired using an Olympus BX60 Microscope (Olympus Corporation, Japan) by investigators blinded to the grouping methods. We randomly selected five regions in each rat to count Nissl-positive neurons in the anterior horn using Image-Pro Plus 6.0.

Immunofluorescence

For immunofluorescence staining, the slides were deparaffinized, rehydrated, rinsed with PBS three times for 5 min each, antigen repaired using antigen retrieval solution (ZKWB, Beijing, China) for 15 min in a microwave oven, and incubated with 3% hydrogen peroxide for 30 min at room temperature to block endogenous peroxidases. The slides were blocked with 3% BSA (Solarbio, Beijing, China) for 30 min and incubated at 4°C overnight with the following primary antibodies: rabbit anti-pp38 with mouse anti-GFAP, anti-OX42, and anti-NeuN. The slides were then incubated with the respective secondary antibodies for 30 min at 37°C in the dark, DAPI (1:1000 dilution, Abcam) for 10 min in the dark, and mounted with antifade mounting medium (ZKWB, Beijing, China). Images were acquired using a KF-PRO -020 scanner (KFBIO). ImageJ was used for the quantitative analysis of positive cells.

Enzyme-Linked Immunosorbent Assay (ELISA)

The levels of IL-6, TNF- α , and MCP-1 were quantified using ELISA kits (ELR-IL6, ELR-TNF α , RayBio, GA, USA; RGB-60224R, Rigor Bioscience, Beijing, China) according to the manufacturer's instructions. Molecular Devices Spectra Max M2 (Molecular Devices, CA, USA) was used to measure the OD values at 450 nm. Optical density (OD) values were converted to protein concentration.

Western Blotting

Total protein was isolated from the spinal cord tissue using RIPA buffer with protease and phosphatase inhibitors and quantified using a BCA protein assay kit (KeyGEN Biotech, Jiangsu, China), and 10% SDS-PAGE was used for protein separation. PVDF membranes to which protein transferred were blocked with 5% (w/v) non-fat milk in PBS for 2 h at room temperature, incubated at 4°C overnight with the following primary antibodies: phospho-p38, p38, phospho-JNK, JNK, phospho-ERK, ERK, and GAPDH, then incubated at room temperature for 1 h with the respective secondary antibodies. Due to the impact of COVID-19, this part was completed in two laboratories. For phospho-p38, p38, phospho-ERK, ERK, and the corresponding GAPDH, a ECL chemiluminescence detection kit (NCM, Jiangsu, China) and the ChemiDoc MP Imaging System (Bio-Rad, CA, USA) were used to visualize the bands. For phospho-JNK, JNK, and the corresponding GAPDH, Western Lightning Plus-ECL (Perkin Elmer, MA, USA) and Kodak XBT-1 film (Kodak, NY, USA) were used to visualize the bands. It should be noted that, for each MAPK, the order of “phospho-MAPK bands, stripping & re-blocking, MAPK bands, stripping & re-blocking, GAPDH bands” was followed, and stripping buffer (Aoqing Biotech, Beijing, China) was used to strip the previous bands. Finally, the gray value and relative expression levels of each band were obtained using ImageJ software to calculate the phosphorylation ratio of each MAPK (phospho-MAPK/MAPK \times 100%).

Statistical Analysis

SPSS 22.0 (IBM, Armonk, NY, USA) was used to analyze the data. All data are expressed as the mean \pm standard error of the mean (SEM). Comparisons between groups were made using one-way analysis of variance, followed by the least significant difference test for post-hoc comparisons. $P < 0.05$ was regarded as statistically significant.

Results

Effects of IQAB on Neurobehavioral Tests of CSR Rats

For 50% PWMT, no significant change was observed in the control group throughout the experimental process. No significant differences were observed between the sham and control groups at any time point ($P > 0.05$). The model group recovered slowly and was still significantly lower than the sham group on day 14 ($P < 0.01$). The Fenbid, LEA, and IQAB groups showed an upward trend; however, only on day 14, when the 50% PWMT of these three groups was significantly higher than that of the model group ($P < 0.05$). On days 7, 10, and 14, the 50% PWMT in the IQAB group was higher than that in the LEA group; however, the differences were not statistically significant ($P > 0.05$) (Figure 3A).

For gait evaluation using Kawakami's method, both the control and sham groups remained at a low score throughout the process. The gait score of the model group was significantly higher than that of the sham group at each time point, even on day 14 ($P < 0.01$). On day 10, the gait score of the Fenbid group was significantly lower than that of the model group ($P < 0.05$). On day 14, the gait scores of the Fenbid ($P < 0.01$), LEA ($P < 0.05$), and IQAB ($P < 0.01$) groups were lower than those of the model group. The Fenbid and IQAB groups had lower scores than the LEA group on days 10 and 14, but there were no significant differences between these three groups ($P > 0.05$) (Figure 3B).

Effects of IQAB on Spinal Histological Changes of CSR Rats

No significant pathological changes were observed in the control or sham groups. Compared with the sham group, HE staining of the spinal cord showed more necrotic foci and fewer motoneurons on the compression side of the model group. Edema was more severe in the model group, as indicated by the obvious vacuolar changes in the neurons. Compared with the model group, the Fenbid, LEA, and IQAB groups had fewer necrotic foci and vacuolar changes.

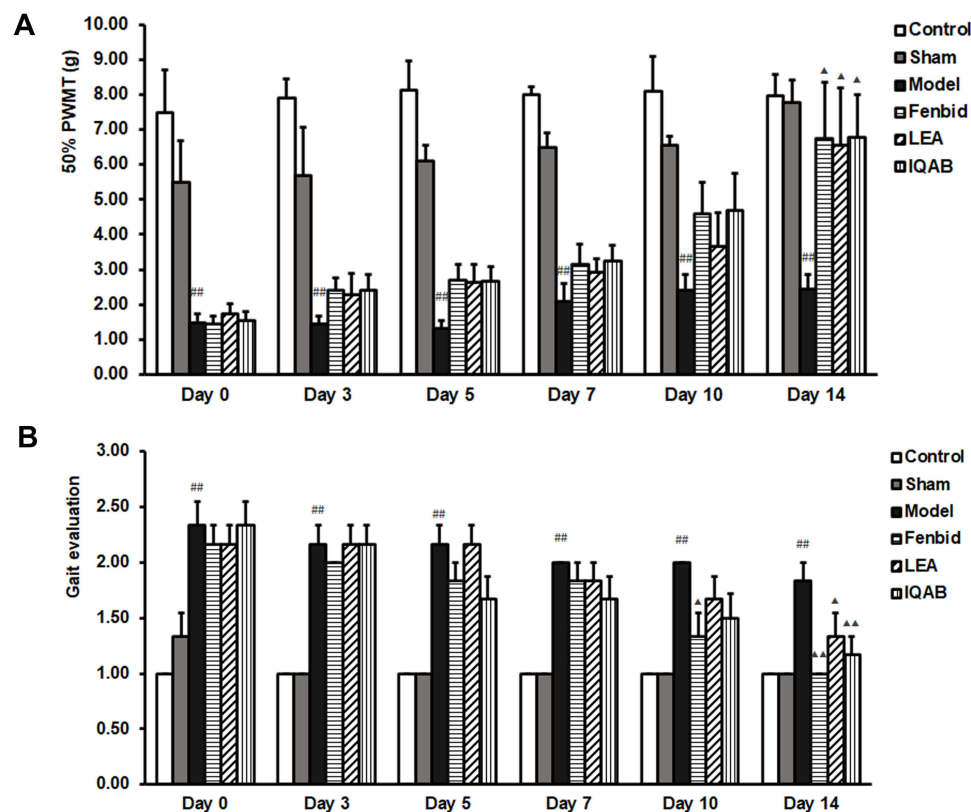


Figure 3 Effect of IQAB on neurobehavioral tests of CSR rats.

Notes: (A) 50% PWMT in the six groups. (B) Gait evaluation using Kawakami's method. Compared with the model group, IQAB significantly reduced mechanical allodynia ($P < 0.05$) and poor gait evaluation ($P < 0.01$) at D14. Mean \pm SEM, $n = 6$. ### $P < 0.01$ versus the sham group; $\Delta P < 0.05$, $\Delta\Delta P < 0.01$ versus the model group.

Abbreviations: PWMT, paw withdrawal mechanical threshold; LEA, local electroacupuncture; IQAB, "Invigorating Qi and activating Blood".

Among the three groups that received the intervention, IQAB most markedly improved the histological changes (Figure 4A).

Nissl staining showed that the Nissl bodies were deeply stained in the ventral horn of the compressing side of the control and sham groups. The neurons were arranged in good order, and there was no Nissl body missing area. In the model group, Nissl bodies were stained with low intensity, neurons were sparsely arranged, and some areas of the Nissl bodies were missing. In the three groups that received interventions, the staining intensity of Nissl bodies, distribution of neurons, and missing areas of Nissl bodies were modified to different extents, which were more obvious in the Fenbid and IQAB groups (Figure 4B). Furthermore, there was no significant difference in the number of Nissl-positive cells between the control and sham groups ($P > 0.05$); however, the number of Nissl-positive cells in the model group was significantly lower than in the sham group ($P < 0.05$); the figure for the IQAB group was significantly higher than that in the model group ($P < 0.05$) (Figure 4C).

Effects of IQAB on IL-6 and TNF- α Levels in Spinal Cord of CSR Rats

ELISA results showed that the level of IL-6 in the spinal cord of the model group was significantly higher than that in the sham group ($P < 0.01$). Compared with the model group, the level of IL-6 in the spinal cord of all three groups decreased, but only LEA ($P < 0.05$) and IQAB ($P < 0.01$) were statistically significant (Figure 5A). In addition, the IL-6 levels in the IQAB group were significantly lower than those in the Fenbid group ($P < 0.05$). The TNF- α levels in the spinal cord were significantly higher in the model group than in the sham group ($P < 0.05$). Compared with the model group, TNF- α levels in all three groups were significantly decreased, but only LEA and IQAB were statistically significant ($P < 0.01$) (Figure 5B). In addition, there were no significant differences among the three groups that received the intervention ($P > 0.05$).

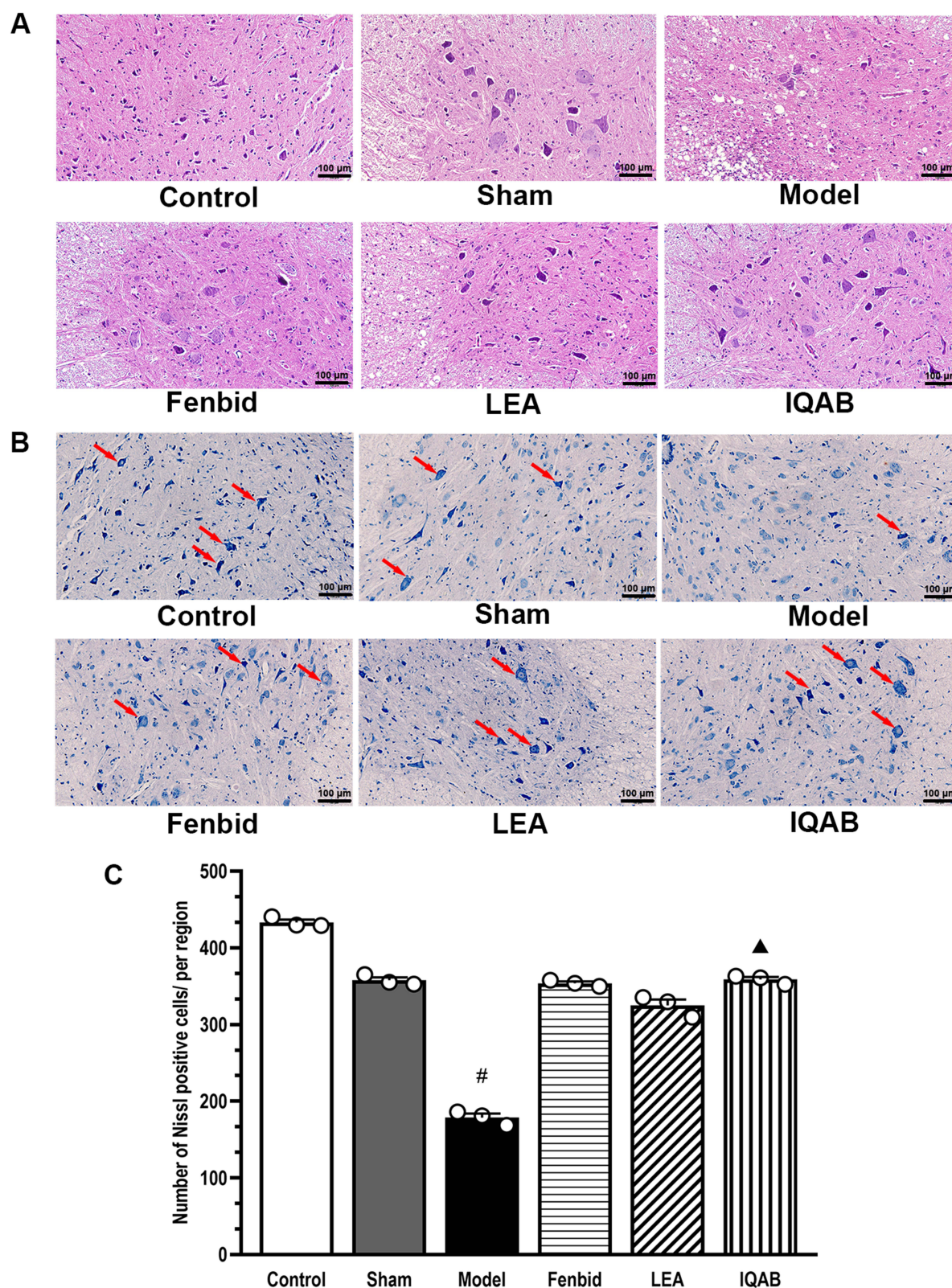


Figure 4 Effects of IQAB on spinal histological changes of CSR rats.

Notes: (A) HE staining ($\times 200$), IQAB could modify necrosis foci, neuron edema, and motoneuron loss on the compression side of the spinal cord of CSR rats. (B and C) Nissl staining ($\times 200$). IQAB significantly increased Nissl-positive neurons (red arrows) in the compression side of the spinal cord of CSR rats ($P < 0.05$), suggesting regulation of neuronal apoptosis. Scale bar: 100 μm . Mean \pm SEM, $n = 3$ for animal numbers, $n = 5$ for the number of fields of view for each animal. # $P < 0.05$, versus sham group; ▲ $P < 0.05$, versus model group.

Abbreviations: LEA, local electroacupuncture; IQAB, “Invigorating Qi and activating Blood” acupuncture.

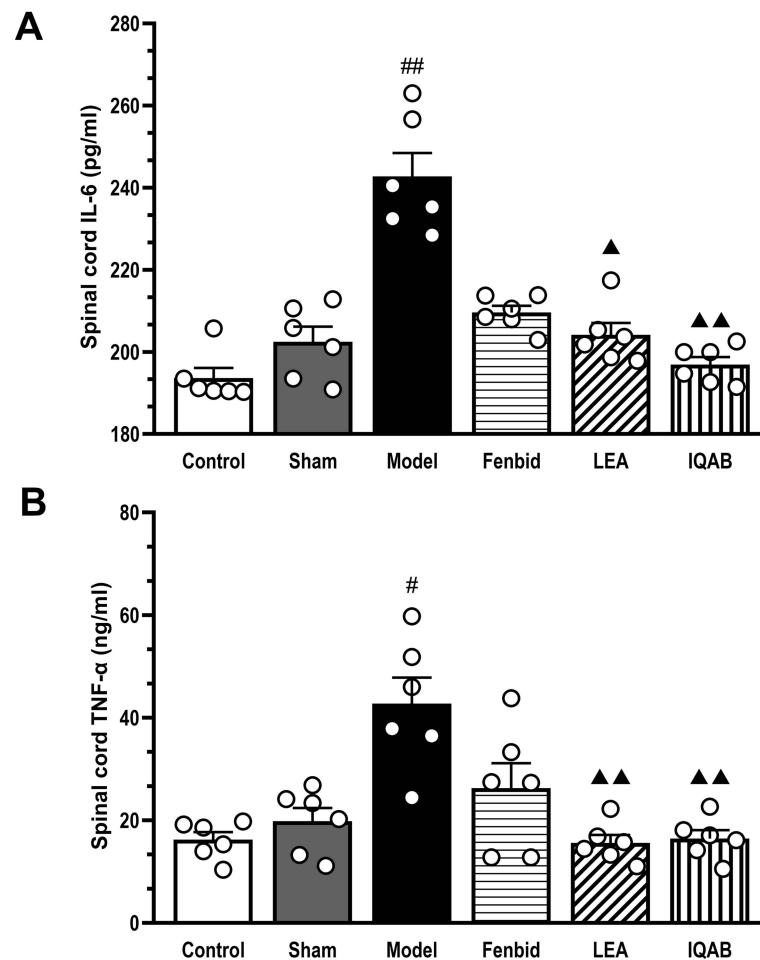


Figure 5 Effects of IQAB on IL-6 and TNF- α levels in spinal cord of CSR rats.

Notes: (A) IL-6 levels in the spinal cord. (B) TNF- α level in the spinal cord. The levels of IL-6 and TNF- α were significantly increased in the model group ($P < 0.01$ or $P < 0.05$, versus the sham group) and decreased in the IQAB group ($P < 0.01$ versus model group). Mean \pm SEM, $n = 6$. [#] $P < 0.05$, ^{##} $P < 0.01$, versus sham group; [▲] $P < 0.05$, ^{▲▲} $P < 0.01$ versus model group.

Abbreviations: IL-6, interleukin-6; TNF- α , tumor necrosis factor- α ; LEA, local electroacupuncture; IQAB, “Invigorating Qi and activating Blood”.

Effects of IQAB on MAPKs Phosphorylation Ratio of CSR Rats

Western blotting results showed that the phosphorylation ratio of p38 (p-p38/p38) in the spinal cord of the compression segment in the model group was significantly higher than that in the sham group ($P < 0.01$). Compared with the model group, it decreased significantly in the IQAB group ($P < 0.01$) (Figure 6A and B). The phosphorylation ratio of ERK (p-ERK/ERK) in the spinal cord of the compression segment in the model group was higher than that in the sham group; however, the difference was not statistically significant ($P > 0.05$). Compared with the model group, the phosphorylation ratio of ERK was significantly decreased in the IQAB group ($P < 0.01$) (Figure 6C and D). The phosphorylation ratio of JNK (p-JNK/JNK) in the model group was significantly higher than that in the sham group ($P < 0.01$). Compared with the model group, the phosphorylation ratio of JNK in the IQAB group was lower, but no statistical difference was observed ($P > 0.05$) (Figure 6E and F). Furthermore, the immunofluorescence results for p-p38 in the left cervical spinal cord showed that the average fluorescence intensity of p-p38 in the model group was significantly stronger than that in the sham group ($P < 0.01$), whereas that in the IQAB group was significantly lower than that in the model group ($P < 0.01$) (Figure 6G and H).

Effects of IQAB on p-p38 Activities in Certain Cell Types in Spinal Cord of CSR Rats

The results of co-labeling immunofluorescence showed that, in the model group, colocalization of p-p38+NeuN and p-p38+OX42 in the compressing-side spinal cord per region was significantly higher than that in the sham group ($P < 0.01$), but colocalization of

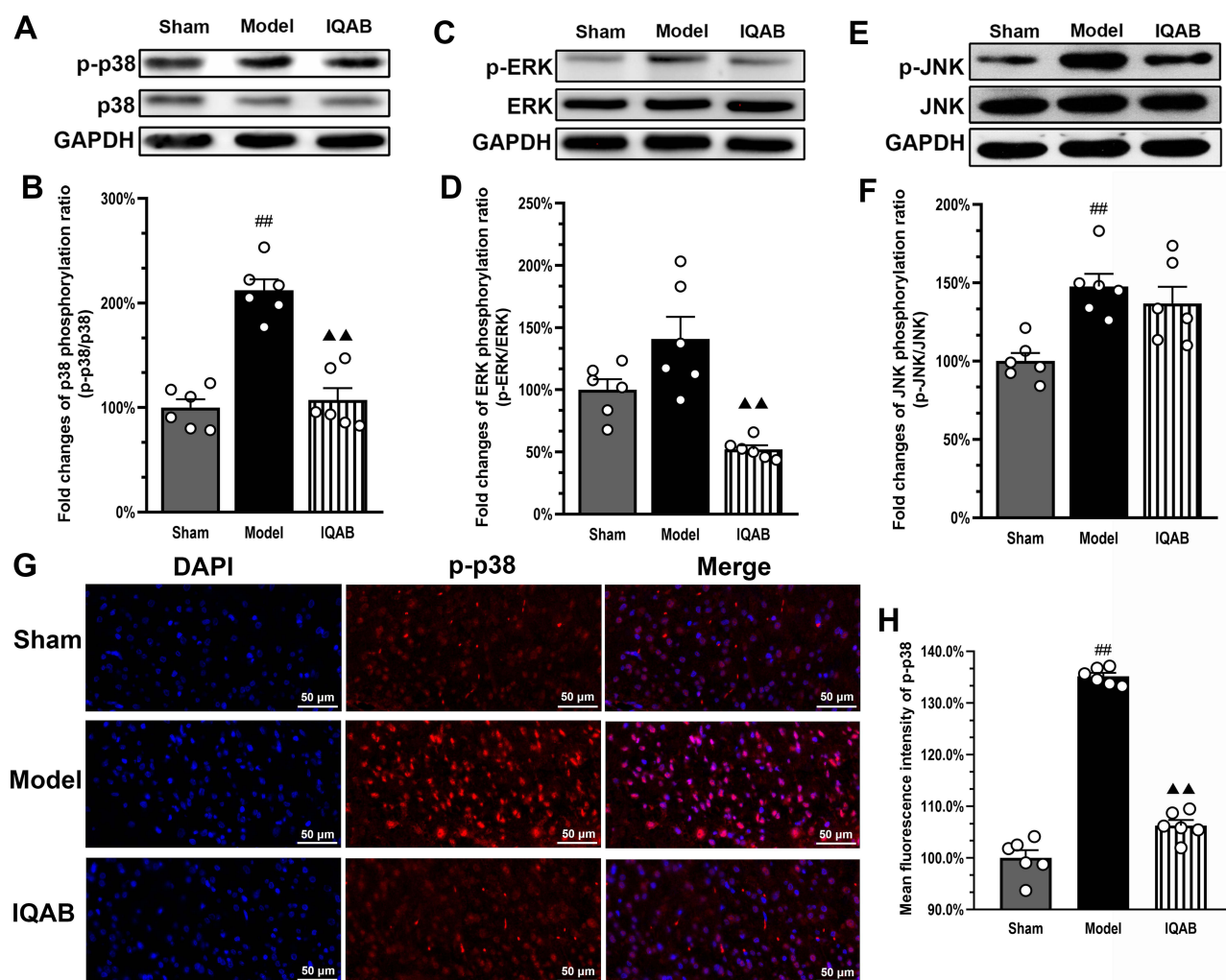


Figure 6 Effects of IQAB on MAPK pathway changes of CSR rats.

Notes: Western blot results for p-p38/p38 (**A** and **B**), p-ERK/ERK (**C** and **D**), and p-JNK/JNK (**E** and **F**) in the cervical spinal cords. Compared with the model group, IQAB significantly reduced the phosphorylation ratio of p38 and ERK ($P < 0.01$). (**G** and **H**) Immunofluorescence results for p-p38 in the compression-side cervical spinal cord showed that the average fluorescence intensity of p-p38 was significantly reduced by IQAB ($P < 0.01$). Scale bar: 50 μ m. Mean \pm SEM, $n = 6$ for number of animals (**A–F**) and number of view fields for each group (**G** and **H**). ^{##} $P < 0.01$ versus sham group; ^{▲▲} $P < 0.01$ versus model group.

Abbreviations: ERK, extracellular regulated protein kinase; JNK, c-Jun N-terminal kinase; IQAB, “Invigorating Qi and activating Blood”.

p-p38+GFAP was lower than that in the sham group ($P < 0.01$). Compared to the model group, the colocalization of p-p38+NeuN and p-p38+OX42 in the IQAB group was significantly lower ($P < 0.05$), but the colocalization of p-p38+GFAP was not statistically different ($P > 0.05$) (Figure 7A–F).

Effects of IQAB on Level of MCP-1 in Spinal Cord of CSR Rats

ELISA results showed that the level of MCP-1 in the spinal cord of the model group was significantly higher than that in the sham group ($P < 0.05$). Compared with the model group, the level of MCP-1 in the spinal cord of the IQAB group was significantly lower ($P < 0.01$) (Figure 8).

Discussion

Radicular pain caused by CSR is a type of NP and the occurrence of allodynia is a characteristic manifestation. Allodynia refers to pain caused by stimuli that usually do not cause pain, which represents the impairment of the nociceptive system’s formal function to “separating” harmful and non-harmful information.^{31,32} The mechanical threshold is a quantification of allodynia, and the Kawakami score is a straightforward quantitative method for gait. In our research,

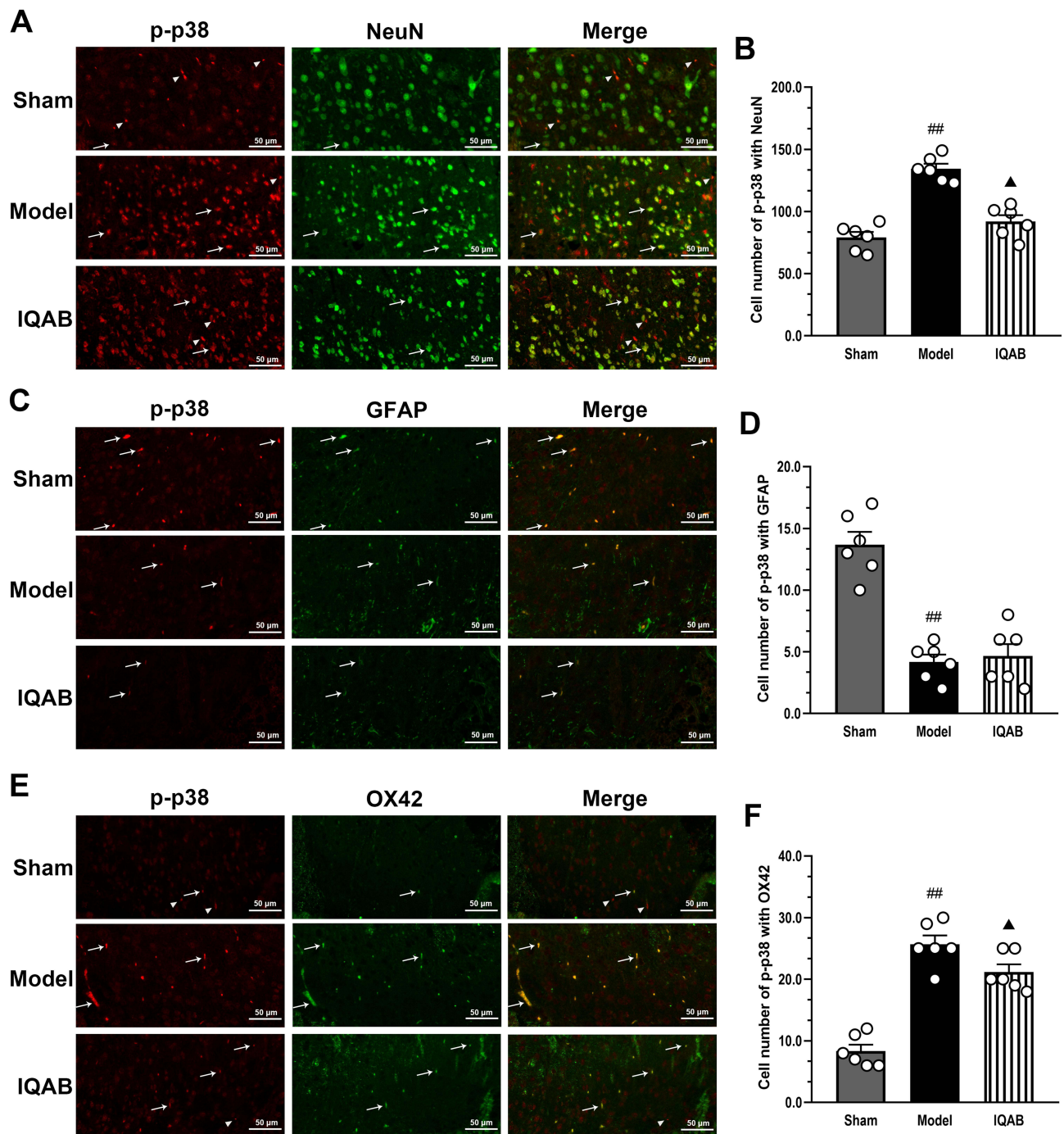


Figure 7 Effects of IQAB on p-p38 activities in certain cell types of CSR rats.

Notes: Co-labeling with p-p38+NeuN (**A** and **B**), p-p38+GFAP (**C** and **D**) and p-p38+OX42 (**E** and **F**) in the spinal cord. Co-labeling with p-p38+NeuN and p-p38+OX42 ($P < 0.05$), but not with p-p38+GFAP ($P > 0.05$), was downregulated by IQAB. Scale bar: 50 μ m. P-p38-labelled cells that were positive (arrows) or not positive (arrowheads) for the markers. Mean \pm SEM, $n = 6$ for the number of view fields in each group. ^{##} $P < 0.01$ versus sham group; [▲] $P < 0.05$, versus model group.

Abbreviations: GFAP, glial fibrillary acidic protein; OX42, oxycocin-42; IQAB, "Invigorating Qi and activating Blood".

some model rats initially showed severe gait disorder, but the gait was normal after D7, with the forelimb of the affected side often lifted off the ground at rest. Therefore, gait instability may not be caused by the loss of innervation but rather by pain contracture. IQAB significantly improved pain allodynia of the affected forelimb and pain-induced gait instability, with an effect comparable to that of Fenbid, and demonstrated a trend toward better improvement than LEA.

Previous studies utilizing this modeling method showed that on the 7th day after surgery, the spinal cord showed neuronal edema with cytolysis and necrosis and a decreased number of neurons and even regions of loss.³³ This indicates

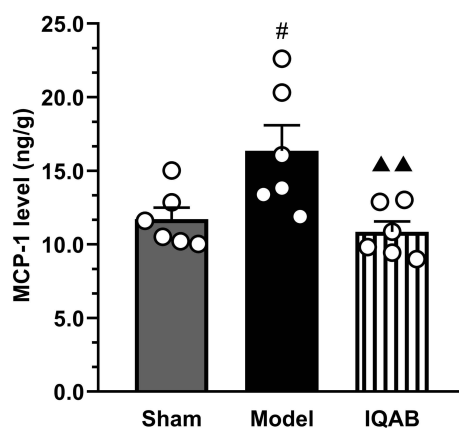


Figure 8 Effects of IQAB on MCP-1 level in spinal cord of CSR rats.

Notes: The levels of MCP-1 in the spinal cord significantly increased in the model group ($P < 0.05$) and decreased in the IQAB group ($P < 0.01$). Mean \pm SEM, $n = 6$. # $P < 0.05$, versus the sham group; ▲▲ $P < 0.01$ versus the model group.

Abbreviations: MCP-1, monocyte chemoattractant protein-1; IQAB, “Invigorating Qi and activating Blood” acupuncture.

that the neuronal cell membrane has been damaged, its permeability is increased, and the distribution and function of transmembrane ionized channels and their receptors are affected, facilitating or maintaining pain through abnormal discharge. To further observe the changes in neurons, more specific Nissl staining was performed. Nissl bodies of neurons in the anterior horn of the spinal cord could be sporadically distributed and small in shape, on the 14th day after operation, which is speculated to be related to the impairment of motor function of the forelimbs.³⁴ In this study, the above pathological changes were similar to those studies. IQAB had a significant effect in repairing inflammatory edema of the spinal cord and damage to anterior horn neurons; Both Fenbid and LEA also showed a similar trend but revealed no statistical significance in the reduction of Nissl-positive neuron counts.

IL-6 and TNF- α are the cytokines that promote the development and chronicity of NP. IL-6 inhibition reduces hyperalgesia and allodynia in NP models. TNF- α can regulate acute and chronic inflammation to help the body restore balance, but excessive secretion of TNF- α may cause inflammation maintenance and cell dysfunction.³⁵ Both cytokine levels in CSR rats’ spinal cord were significantly higher than in the sham group, indicating that the local inflammatory effect was obvious. IQAB significantly reduced the levels of both cytokines, but there was no significant difference compared with LEA. Previous studies have shown that ibuprofen mainly exerts analgesic effects by inhibiting the synthesis of prostaglandins, but also downregulating of systemic inflammatory biomarkers such as IL-6 in serum of NP patients.³⁶ In this study, ibuprofen showed a trend of reducing the levels of two cytokines in the spinal cord, but there was no significant difference compared to the model group. This may be related to the small sample size and need to be clarified in further investigation.

Having clarified the protective effect of IQAB, we explored its effect on the phosphorylation of three MAPK proteins in the spinal cord. Elevation of proinflammatory cytokines, such as IL-6 and TNF- α , is a factor that induces MAPKs phosphorylation. Phosphorylated MAPKs can promote the production of neuromodulators, including these cytokines, in turn, to form damaging effects. Specifically, two of JNK subtypes, JNK1 and JNK2, express extensively in the spinal cord. As for the active form, pJNK1 (p46) is the main expression form in the spinal cord, its expression increases after nerve injury, being activated by upstream factors such as IL-1, TNF- α and fibroblast growth factor-2.³⁷ In spinal nerve ligation model, JNK activation in the spinal cord can last for more than three weeks.³⁸ Its downstream mechanisms include astrocytic JNK-HDAC2 cascade that contributes to GLT-1 decrease, or being translocated to the nucleus to phosphorylate many nuclear substrates (mostly transcription factors), thereby causing sensitization of pain.³⁹ There are almost no p-ERK positive cells in the spinal dorsal horn neurons of unstimulated animals, and ERK in the spinal dorsal horn neurons of animals can be activated under noxious stimuli that may cause sustained changes in pain sensitivity.¹⁸ Its downstream mechanisms include transcriptional regulation and regulation of ion channels, causing the induction and maintenance of NP. There is a moderate level of basal p-p38 positive cells in the spinal cord. Under nociceptive

stimulation, p-p38 can significantly increase and remain at a high level after 3 weeks. Intrathecal injection of p38 inhibitors can alleviate NP.⁴⁰ For the CSR model used in this experiment, after 17 days persistent stimulation, compared with the sham group, the phosphorylation ratios of p38 and JNK in the model group increased significantly, while the trend for a higher phosphorylation ratio of ERK was not statistically significant. IQAB significantly inhibited p38 and ERK phosphorylation. Although the phosphorylation rate of JNK also decreased after IQAB intervention, this difference was not statistically significant. This indicates that IQAB primarily exerts therapeutic effects by affecting the p38 among three MAPKs. Then we investigated the distribution of its phosphorylated form in the spinal cord by immunofluorescence and found that p-p38 was mainly present in the gray matter. The mean fluorescence intensity was also significantly enhanced in the model group and significantly reduced after IQAB intervention. Therefore, we explored the mechanisms by which IQAB modulated the activation of p38 in spinal gray matter.

First, we identified specific cell types in which IQAB-regulated p38 activation was predominant. At the cellular level, non-neuronal cells are increasingly being recognized as playing a critical role in chronic pain processing, particularly in glia, which can directly release multiple neuromodulators. In different NP models, the activated form of p38 was present in different spinal glia: astrocytes, in the partial sciatic nerve ligation model; microglia, in the spared nerve injury model; both, in the spinal cord injury model.^{41–43} In this CSR model prepared by inserting compressive foreign matter, p-p38 was significantly elevated in spinal neurons and microglia, but not in astrocytes; p-p38 was significantly reduced at D14 in both neurons and microglia after IQAB intervention. It has been reported that microglia can be activated in a polarization manner into M1 and M2 types, and M1 can release proinflammatory substances such as iNOS, IL-6, IL-1 β , and TNF- α ; M2 can produce anti-inflammatory factors such as IL-4 and IL-10.⁴⁴ Both types increase in the spinal cord at the early stage after nerve injury, and the M1/M2 ratio gradually increases in later stages after injury, gradually diminishing to a single M1 expression.⁴⁵ This imbalance in polarization may explain the occurrence and chronicity of NP. There is evidence that electroacupuncture can polarize microglia toward the M2 phenotype, thereby delaying neurodegeneration in AD rats.⁴⁶ Whether IQAB can exert protective effects in a similar way of regulating microglia polarization is left for further investigation.

We then observed the effects of IQAB on MCP-1 levels in the spinal cord. The results showed that p-p38 expression in both spinal neurons and microglia was downregulated by IQAB, suggesting that IQAB may be involved in the regulation of neuron–microglia interactions. Among the neuromodulators downstream of p38, chemokines may not only participate in the formation of central sensitization by increasing presynaptic transmitters, but also act as signaling molecules by activating their receptors on other types of cells.⁴⁷ MCP-1 is one of these chemokines that plays a key role in neuron–glia interactions. In some NP models, MCP-1 can be transmitted from primary neurons in the dorsal root ganglion to the spinal cord dorsal horn, then bind to its receptor CCR2 on microglia, causing p38 phosphorylation there, promoting inflammatory cytokine production, and triggering central sensitization; or can be activated by TNF- α produced by p38-mediated microglial activation, then expressed in astrocytes, activating CCR2 on spinal neurons, and inducing central sensitization.⁴⁸ IQAB significantly reduced the abnormally elevated MCP-1 level, which may be one of the pathways that IQAB regulates neuron–microglia interactions in the spinal cord of CSR rats.

In the two distal adjunct points, ST36 is a key acupoint for invigorating *Qi* based on its relation to the stomach and spleen via the Stomach Meridian Foot-*Yangming*. This makes it useful not only for gastrointestinal diseases, but also for a wide variety of pain with *Qi* disorders, such as osteoarthritis, peri-arthritis, and sciatica. Recent studies have found that electroacupuncture at ST36 could produce analgesic effects by reducing tyrosine kinase B receptor and microglial activation-induced BDNF in the spinal cord of rats with chronic constrictive injury.^{49,50} As a Back-*shu* acupoint, BL17 belongs to the Bladder Meridian Foot-*Taiyang* and is located between the *Heart* and *Liver* Back-*shu* points. Both viscera are important for regulating the *Blood* state. That makes BL17 become “Xuehui” (*Blood* influential point) in “eight influential points”, and is often used in *Blood* stasis syndromes of diseases like lumbar disc herniation, diabetes peripheral neuropathy, and hypertension. In the vascular dementia model, electroacupuncture at BL17 has a neuroprotective effect by reducing p38-induced neuronal apoptosis in the hippocampus.⁵¹ Although often used, it shows some analgesic and neuroprotective effects in several animal models, which are very limited in experimental data of CSR. The advantages of IQAB in this research indicate that future experimental studies on acupuncture interventions for CSR may not only explore the anti-radiculopathy effects of local acupoints but should also try other acupuncture

schedules that are based on TCM theory and clinical practice, thereby providing more realistic evidence for TCM therapy options for CSR.

In this study, IQAB showed better trends than LEA in relieving pain and reducing the inflammatory level in spinal cord neurons, but the difference was not statistically significant. This may be related to the sample size, overall duration, and specific indicators used in the experiment. In the future, it will be necessary to test the therapeutic effect of IQAB using a larger sample size, different CSR stages, and detection indicators that better reflect the state of *Qi* and *Blood* such as microcirculation and motor scores. Furthermore, we selected p38 to identify the specific cell types that are highly activated; however, how other MAPKs participate in the curative effects of IQAB at the cellular level remains unclear. We also found that IQAB could influence p38 activation in microglia and neurons and decrease the chemokine MCP-1; however, the specific mechanism by which it regulates this MCP-1 related microglia–neuron interaction is unknown. These two aspects should be explored further in future studies.

Conclusion

In summary, we conclude that IQAB alleviates neuropathic pain, improves the pathological changes and abnormal level of inflammatory cytokines in spinal cord. These effects are related to inhibition of the spinal microglia activation mediated by p38 activation, and the regulation of the neuron-microglia interaction mediated by MCP-1. These findings provide new insights into potential therapeutic targets of acupuncture in CSR therapy.

Funding

This research was supported by the National Natural Science Foundation of China (No. 82174505) and the University Transverse Development Fund of Beijing University of Chinese Medicine (No. 2030071720017). Funding support did not affect the statistical analysis of objective data or their reports.

Disclosure

The authors report no conflicts of interest in this work.

References

1. GBD 2015 DALYs and HALE Collaborators. Global, regional, and national disability-adjusted life-years (DALYs) for 315 diseases and injuries and healthy life expectancy (HALE), 1990–2015: a systematic analysis for the Global Burden of Disease Study 2015. *Lancet*. 2016;388(10053):1603–1658. doi:10.1016/S0140-6736(16)31460-X
2. Xu JH. *Epidemiological investigation of cervical spondylosis in Shanghai urban population and clinical study on treatment of cervical spondylotic radiculopathy with JinBi Granules* [Doctoral]. Shanghai University of Traditional Chinese Medicine; 2019.
3. Bono CM, Ghiselli G, Gilbert TJ, et al. An evidence-based clinical guideline for the diagnosis and treatment of cervical radiculopathy from degenerative disorders. *Spine J*. 2011;11(1):64–72. doi:10.1016/j.spinee.2010.10.023
4. Zhang RL, You Z, Wang R. Analyze the clinical effect of acupuncture and moxibustion in the treatment of cervical spondylotic radiculopathy with sleep disorders. *World J Sleep Med*. 2021;8(10):1707–1708.
5. Rhee JM, Yoon T, Riew KD. Cervical radiculopathy. *J Am Acad Orthop Surg*. 2007;15(8):486–494. doi:10.5435/00124635-200708000-00005
6. Thoomes EJ. Effectiveness of manual therapy for cervical radiculopathy, a review. *Chiropr Man Therap*. 2016;24(1):45. doi:10.1186/s12998-016-0126-7
7. Kjaer P, Kongsted A, Hartvigsen J, et al. National clinical guidelines for non-surgical treatment of patients with recent onset neck pain or cervical radiculopathy. *Eur Spine J*. 2017;26(9):2242–2257. doi:10.1007/s00586-017-5121-8
8. Cheng CH, Tsai LC, Chung HC, et al. Exercise training for non-operative and post-operative patient with cervical radiculopathy: a literature review. *J Phys Ther Sci*. 2015;27(9):3011–3018. doi:10.1589/jpts.27.3011
9. Nakajima M, Inoue M, Itoi M, Kitakoji H. Clinical effect of acupuncture on cervical spondylotic radiculopathy: results of a case series. *Acupunct Med*. 2013;31(4):364–367. doi:10.1136/acupmed-2013-010317
10. China Association of Acupuncture and Moxibustion. *Evidence-Based Guidelines for Clinical Practice with Acupuncture and Moxibustion: Cervical Spondylosis of Nerve Root Type*. Beijing: China Press of Traditional Chinese Medicine Co., Ltd.; 2015.
11. Wang LL, Li M, Jin F, Wang SZ. Study on effects and mechanism of electro-acupuncture at Jiaji points on radicular neuralgia in rats with cervical spondylotic radiculopathy. *J Liaoning Univ Tradit Chin Med*. 2014;16(6):111–114.
12. Huang X, Su SY, Chen S, et al. Study on analgesic mechanism of electroacupuncture on CSR rats based on ERK signaling pathway. *Chin Arch Tradit Chin Med*. 2020;38(2):195–198,291.
13. Yang S, Meng L, Zhong QH, Jiang XY. Effect of electro-needling cervical Jiaji points on expressions of GFAP, NF-κB and inflammatory cytokines in spinal dorsal horn of rats with neuropathic pain of CSR. *J Clin Acupunct Moxibustion*. 2022;38(1):70–75.
14. Zhou JW, Pi Y, Yan P. Study on the distribution of TCM syndromes in 660 patients with CSR. *J Sichuan Tradit Chin Med*. 2012;30(6):69–70.
15. Woods BI, Hilibrand AS. Cervical radiculopathy: epidemiology, etiology, diagnosis, and treatment. *J Spinal Disord Tech*. 2015;28(5):E251–E259. doi:10.1097/BSD.0000000000000284

16. van Boxem K, Huntoon M, van Zundert J, Patijn J, van Kleef M, Joosten EA. Pulsed radiofrequency: a review of the basic science as applied to the pathophysiology of radicular pain: a call for clinical translation. *Reg Anesth Pain Med*. 2014;39(2):149–159. doi:10.1097/AAP.0000000000000063
17. Leung L, Cahill CM. TNF-alpha and neuropathic pain—a review. *J Neuroinflammation*. 2010;7(1):27. doi:10.1186/1742-2094-7-27
18. Ji RR, Gereau RW, Malcangio M, Strichartz GR. MAP kinase and pain. *Brain Res Rev*. 2009;60(1):135–148. doi:10.1016/j.brainresrev.2008.12.011
19. Inoue K. The function of microglia through purinergic receptors: neuropathic pain and cytokine release. *Pharmacol Ther*. 2006;109(1–2):210–226. doi:10.1016/j.pharmthera.2005.07.001
20. Seki S, Sekiguchi M, Konno SI. Association between neurotrophic factor expression and pain-related behavior induced by nucleus pulposus applied to rat nerve root. *Spine*. 2018;43(1):E7–E15. doi:10.1097/BRS.0000000000002223
21. Wang G, Huang C, Wang Y, Guo Q, Jiang H, Wen J. Changes in expression of cyclooxygenase-2 in the spinal dorsal horn after intrathecal p38MAPK inhibitor SB203580 on neuropathic pain in rats. *Ann Palliat Med*. 2013;2(3):124–129. doi:10.3978/j.issn.2224-5820.2013.07.02
22. Limcharoen T, Muangnoi C, Dasuni Wasana PW, et al. Improved antiallodynic, antihyperalgesic and anti-inflammatory response achieved through potential prodrug of curcumin, curcumin diethyl diglutarate in a mouse model of neuropathic pain. *Eur J Pharmacol*. 2021;899:174008. doi:10.1016/j.ejphar.2021.174008
23. Gao YJ, Zhang L, Samad OA, et al. JNK-induced MCP-1 production in spinal cord astrocytes contributes to central sensitization and neuropathic pain. *J Neurosci*. 2009;29(13):4096–4108. doi:10.1523/JNEUROSCI.3623-08.2009
24. Zhao J, Su SY, Chen X, et al. Effects of electroacupuncture distal acupoints on analgesic factors of cervical spondylosis radiculopathy model's rats. *J Liaoning Univ Tradit Chin Med*. 2018;20(11):179–182.
25. Tian Y, Zhang J, Jiang XY. Effect of electroacupuncture at 1 cun to the left or right side of cervical Jiaji points on tumor necrosis factor- α in rats with cervical spondylotic radiculopathy. *Hunan J Tradit Chin Med*. 2017;33(5):169–171.
26. Lee JY, Choi DC, Oh TH, Yune TY. Analgesic effect of acupuncture is mediated via inhibition of JNK activation in astrocytes after spinal cord injury. *PLoS One*. 2013;8(9):e73948. doi:10.1371/journal.pone.0073948
27. Li SS, Tu WZ, Zhong YB, Jiang X, Jiang SH. Involvement of central neuroglia cells in analgesic effect of electroacupuncture therapy for neuropathic pain. *Acupunct Res*. 2016;41(4):369–372.
28. Xie W, Zhao WH, Yu L, Bao Y. Study on effects and mechanism of extract of Rhizoma Chuanxiong on radicular neuralgia in rats with cervical spondylotic radiculopathy. *J Guangdong Coll Pharm*. 2008;24(5):496–499.
29. Chaplan SR, Bach FW, Pogrel JW, Chung JM, Yaksh TL. Quantitative assessment of tactile allodynia in the rat paw. *J Neurosci Methods*. 1994;53(1):55–63. doi:10.1016/0165-0270(94)90144-9
30. Kawakami M, Weinstein JN, Spratt KF, et al. Experimental lumbar radiculopathy. Immunohistochemical and quantitative demonstrations of pain induced by lumbar nerve root irritation of the rat. *Spine*. 1994;19(16):1780–1794. doi:10.1097/00007632-199408150-00001
31. He Y, Kim PY. Allodynia. In: *StatPearls*. StatPearls Publishing LLC; 2023.
32. Jensen TS, Finnerup NB. Allodynia and hyperalgesia in neuropathic pain: clinical manifestations and mechanisms. *Lancet Neurol*. 2014;13(9):924–935. doi:10.1016/S1474-4422(14)70102-4
33. Wu DW, He J. Effect of Shaoyao Gancao Decoction on the level of inflammatory factors in rats with acute cervical spondylotic radiculopathy. *Asia-Pacific J Tradit Med*. 2018;14(12):9–13.
34. Lai SM. *Effect of Puerarin on PI3K/AKT signaling pathway in cervical spondylotic radiculopathy* [Master]. Guangdong Pharmaceutical University; 2018.
35. Cavalcanti MRM, Passos FRS, Monteiro BS, et al. HPLC-DAD-UV analysis, anti-inflammatory and anti-neuropathic effects of methanolic extract of *Sideritis bilgeriana* (Lamiaceae) by NF-kappaB, TNF-alpha, IL-1beta and IL-6 involvement. *J Ethnopharmacol*. 2021;265:113338. doi:10.1016/j.jep.2020.113338
36. Park A, Anderson D, Battaglini RA, Nguyen N, Morse LR. Ibuprofen use is associated with reduced C-reactive protein and interleukin-6 levels in chronic spinal cord injury. *J Spinal Cord Med*. 2022;45(1):117–125. doi:10.1080/10790268.2020.1773029
37. Ji RR, Kawasaki Y, Zhuang ZY, Wen YR, Decosterd I. Possible role of spinal astrocytes in maintaining chronic pain sensitization: review of current evidence with focus on bFGF/JNK pathway. *Neuron Glia Biol*. 2006;2(4):259–269. doi:10.1017/S1740925X07000403
38. Gao YJ, Ji RR. Activation of JNK pathway in persistent pain. *Neurosci Lett*. 2008;437(3):180–183. doi:10.1016/j.neulet.2008.03.017
39. Lu R, Cui SS, Wang XX, et al. Astrocytic c-Jun N-terminal kinase-histone deacetylase-2 cascade contributes to glutamate transporter-1 decrease and mechanical allodynia following peripheral nerve injury in rats. *Brain Res Bull*. 2021;175:213–223. doi:10.1016/j.brainresbull.2021.07.024
40. Tan L, Hu Y, Zhang X, et al. Corydecumine G inhibits microglia activation via MAPK pathway in a rat model of neuropathic pain. *J Chem Neuroanat*. 2022;124:102124. doi:10.1016/j.jchemneu.2022.102124
41. Xu M, Bruchas MR, Ippolito DL, Gendron L, Chavkin C. Sciatic nerve ligation-induced proliferation of spinal cord astrocytes is mediated by kappa opioid activation of p38 mitogen-activated protein kinase. *J Neurosci*. 2007;27(10):2570–2581. doi:10.1523/JNEUROSCI.3728-06.2007
42. Wen YR, Suter MR, Kawasaki Y, et al. Nerve conduction blockade in the sciatic nerve prevents but does not reverse the activation of p38 mitogen-activated protein kinase in spinal microglia in the rat spared nerve injury model. *Anesthesiology*. 2007;107(2):312–321. doi:10.1097/01.anes.0000270759.11086.e7
43. Crown ED, Gwak YS, Ye Z, Johnson KM, Hulsebosch CE. Activation of p38 MAP kinase is involved in central neuropathic pain following spinal cord injury. *Exp Neurol*. 2008;213(2):257–267. doi:10.1016/j.expneurol.2008.05.025
44. Zhang L, Zhang J, You Z. Switching of the microglial activation phenotype is a possible treatment for depression disorder. *Front Cell Neurosci*. 2018;12:306. doi:10.3389/fncel.2018.00306
45. Xu F, Huang J, He Z, et al. Microglial polarization dynamics in dorsal spinal cord in the early stages following chronic sciatic nerve damage. *Neurosci Lett*. 2016;617:6–13. doi:10.1016/j.neulet.2016.01.038
46. Xie L, Liu Y, Zhang N, et al. Electroacupuncture improves M2 microglia polarization and glia anti-inflammation of hippocampus in alzheimer's disease. *Front Neurosci*. 2021;15:689629. doi:10.3389/fnins.2021.689629
47. Gao YJ, Ji RR. Chemokines, neuronal-glial interactions, and central processing of neuropathic pain. *Pharmacol Ther*. 2010;126(1):56–68. doi:10.1016/j.pharmthera.2010.01.002
48. Ma SB, Xian H, Wu WB, et al. CCL2 facilitates spinal synaptic transmission and pain via interaction with presynaptic CCR2 in spinal nociceptor terminals. *Mol Brain*. 2020;13(1):161. doi:10.1186/s13041-020-00701-6
49. Li SS, Gu PP, Tu WZ, et al. Effects of electroacupuncture on activation of microglia cells in spinal cord in rats with neuropathic pain. *Chin Acupunct Moxibustion*. 2017;37(4):411–416. doi:10.13703/j.0255-2930.2017.04.016

50. Li SS, Tu WZ, Jiang X, et al. Effect of electro-acupuncture at Zusanli (ST36) and Yanglingquan (GB34) acupoint on expression of TrkB receptor in spinal of CCI rats. *Chin Arch Tradit Chin Med*. 2017;35(11):2878–2881.
51. Jia RG. *The experimental study on the influence of different frequency of electroacupuncture on P38MAPK pathway and cell apoptosis of hippocampus in vascular dementia rats* [Master]. Hebei Medical University; 2015.

Journal of Pain Research

Dovepress

Publish your work in this journal

The Journal of Pain Research is an international, peer reviewed, open access, online journal that welcomes laboratory and clinical findings in the fields of pain research and the prevention and management of pain. Original research, reviews, symposium reports, hypothesis formation and commentaries are all considered for publication. The manuscript management system is completely online and includes a very quick and fair peer-review system, which is all easy to use. Visit <http://www.dovepress.com/testimonials.php> to read real quotes from published authors.

Submit your manuscript here: <https://www.dovepress.com/journal-of-pain-research-journal>